

Kinetically Resolved States of the *Halobacterium halobium* Flagellar Motor Switch and Modulation of the Switch by Sensory Rhodopsin I

DONALD A. McCAIN,¹ LOUIS A. AMICI,¹ AND JOHN L. SPUDICH^{1,2*}

Department of Anatomy and Structural Biology¹ and Department of Physiology and Biophysics,² Albert Einstein College of Medicine, Bronx, New York 10461

Received 27 April 1987/Accepted 13 July 1987

Spontaneous switching of the rotation sense of the flagellar motor of the archaeobacterium *Halobacterium halobium* and modulation of the switch by attractant and repellent photostimuli were analyzed by using a computerized cell-tracking system with 67-ms resolution coupled to electronic shutters. The data fit a three-state model of the switch, in which a Poisson process governs the transition from state N (nonreversing) to state R (reversing). After a reversal, the switch returns to state N, passing through an intermediate state I (inactive), which produces a ca. 2-s period of low reversal frequency before the state N Poisson rate is restored. The stochastic nature of the *H. halobium* switch reveals a close similarity to *Escherichia coli* flagellar motor properties as elucidated previously. Sensory modulation of the switch by both photoattractant and photorepellent signals can be interpreted in terms of modulation of the single forward rate constant of the N to R transition. Insight into the mechanism of modulation by the phototaxis receptor sensory rhodopsin I (SR-I) was gained by increasing the lifetime of the principal photointermediate of the SR-I photochemical reaction cycle, S₃₇₃, by replacing the native chromophore, all-*trans*-retinal, with the acyclic analog, 3,7,11-trimethyl-2,4,6,8-dodecapentaenal. Flash photolysis of analog-containing cells revealed an eightfold decrease in the rate of thermal decay of S₃₇₃, and behavioral analysis showed longer periods of reversal suppression than that of cells with the native chromophore over similar ranges of illumination intensities. This indicates that attractant signaling is governed by the lifetime of the S₃₇₃ intermediate rather than by the frequency of photocycling. In this sense, SR-I is similar to rhodopsin, whose function depends on an active photoproduct (Meta-II).

Halobacterium halobium cells swim in a zigzag pattern consisting of linear runs interrupted by spontaneous ca. 180° reversals of swimming direction. Reversals result from switching of the rotation direction of the flagella, which occurs spontaneously at average frequencies of 0.03 to 0.25 s⁻¹ for various strains and culture conditions (1, 14, 25, 29, 30). Modulation of the switch reversal frequency is the basis of phototaxis and chemotaxis by the cells (for reviews, see references 9, 21, and 32).

Changes in light intensity sensed through retinal-containing photoreceptors control the switch to mediate phototaxis responses. An abrupt increase in UV-blue light or decrease in orange-red light is interpreted by the cell as unfavorable, and these stimuli induce reversals of swimming direction. The opposite changes in light intensity suppress reversals. Two photoreceptors have been identified, sensory rhodopsin I (SR-I; λ_{max}, 587 nm (6, 23) and sensory rhodopsin II (SR-II; λ_{max}, 480 nm (20, 32, 34, 35). Photoexcitation of SR-I generates a long-lived intermediate absorbing in the near-UV (λ_{max}, 373 nm), and this species, S₃₇₃, functions as a third phototaxis receptor (23, 31). Attractant light is detected by SR-I₅₈₇ (referred to as SR₅₈₇ below), and repellent light is detected by both S₃₇₃ and SR-II₄₈₀.

The receptor kinetic properties have been studied in detail by flash spectroscopy (6, 23, 33-35). Studies of the output behavioral response have shown complexities of reversal frequency modulation by photostimuli, such as dependence of the magnitude of the response on time after the previous reversal (14) and inversions of the sign of the response depending on background light, strain, stimulus intensity and time after the previous reversal (11, 23, 31, 32, 35). Some

of these effects have been attributed to photoreceptor reactions (e.g., the photochromic states of SR-I and simultaneous stimulation of SR-I and SR-II [23, 31, 32, 35]), and some have been attributed to an endogenous oscillator postulated to control the flagellar motor switch (11, 14, 15).

Mutants have been isolated that produce the apoprotein of SR-I, lack the apoproteins of bacteriorhodopsin and halorhodopsin, contain little or no SR-II apoprotein, and, furthermore, are blocked in retinal synthesis (18, 20, 22). One of these mutants, Flx3R, has been used to incorporate retinal analogs (synthesized in the laboratory of Koji Nakanishi, Columbia University, New York, N.Y.) into SR-I to study chromophore-protein interaction in native membrane vesicles (24) and in vivo (D. A. McCain, L. Amici, C. A. Hasselbacher, and J. L. Spudich, *Biophys. J.* 51:138a, 1987). Wavelength shifts and perturbations of thermal steps in the photochemical reaction cycle of SR-I by specific alterations of the native all-*trans*-retinal have been characterized (24; McCain et al., *Biophys. J.*, 1987). In particular, acyclic and ring desmethyl analogs yield functional SR-I with prolonged lifetimes of the S₃₇₃ intermediate.

The work described here is in two parts. First, we analyze properties of the flagellar motor switch. Second, we use retinal analog perturbation of receptor reactions to study the role of these reactions in modulation of the switch.

MATERIALS AND METHODS

Strains. *H. halobium* Flx3R is a derivative of strain Flx3, which is BR⁻ HR⁻ (18). Flx3R is blocked in retinal synthesis and is nonphototactic. Addition of all-*trans*-retinal generates wild-type amounts of SR-I and restores phototaxis sensitivity (22). Photochemical (20) and behavioral (see Results) analyses indicate a negligible contribution of SR-II to the responses of retinal-reconstituted Flx3R to the repellent light

* Corresponding author.

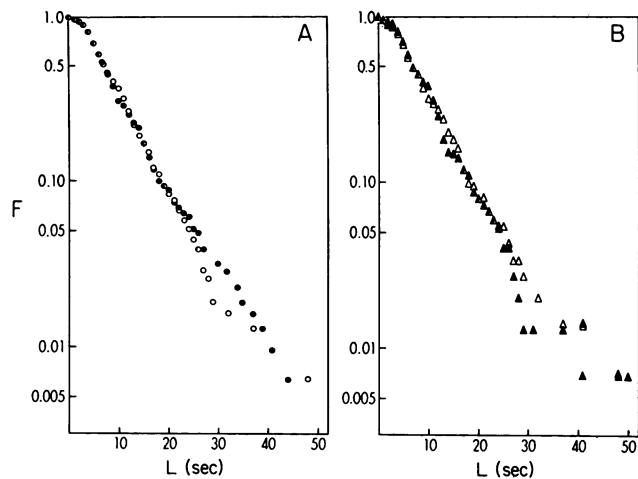


FIG. 1. Spontaneous run length distributions. F is defined as the fractional number of runs of length greater than a given length L , based on 309 runs from 12 individual bacteria of strain Flx3R. (A) Symbols: ●, raw data; ○, same data scaled so that the mean run length of each bacterium equals the ensemble mean (10.4 s). (B) Same data plotted as runs preceded by runs of <8 s (▲, 149 runs) or runs preceded by runs of ≥ 8 s (△, 148 runs).

used (360 to 520 nm), which are attributable to the SR-I two-photon cycle.

Behavioral assay. Cells were grown to late exponential phase in complex medium as described previously (19) and diluted 1:50 into 2 ml of fresh medium, 2 μ l of a 0.8 mM ethanolic solution of all-*trans*-retinal (or retinal analog in the measurements in Fig. 8 and 9) was added, and the suspension was incubated for 2 to 4 h with shaking at 37°C in the dark before behavioral measurements were made. Swimming behavior was monitored at 37°C with nonactinic infrared illumination ($\lambda > 700$ nm), recorded on video tape, and analyzed by using the ExpertVision software on a Sun2/120 work station (Motion Analysis Systems, Inc., Santa Rosa, Calif.) as described (28) or by three-dimensional visual tracking (25) for the data of Fig. 1 and 4. Photostimuli were delivered with the optical arrangement and interference filters described (28). Reversal frequency (F) is calculated as the number of reversals occurring at a particular frame divided by the number of paths present at that frame. Paths containing zero, one, or two reversals are considered in the analysis which used 750 to 1,000 paths per frequency curve.

RESULTS

Spontaneous behavior. The distribution of runs (times between reversals) under nonactinic illumination conditions was determined and is plotted in Fig. 1A (closed circles) as a cumulative distribution as described by Berg and Brown (3). Run lengths are distributed exponentially, except for runs shorter than 2 to 3 s. Normalizing the data so that the mean run length of each cell was made equal to the ensemble mean (Fig. 1A, open circles) did not influence the data to a great extent, except that it brought the 3% tail of longest intervals closer to the exponential fit. The same distribution shape was obtained when previously published spontaneous run length data (14) were plotted in the same manner as Fig. 1. The distributions of runs following long (≥ 8 -s; Fig. 1B, open triangles) or short (<8 -s; Fig. 1B, closed triangles) runs were indistinguishable (Fig. 1B), indicating no persistence of a low or high tendency to reverse from one reversal to the

next. This result confirms the absence of correlation between successive runs reported previously (14).

The spontaneous run length data can be understood in terms of a model for the flagellar motor switch, which is an extension of the model developed by Berg and co-workers (2-5, 16) for *Escherichia coli*, a eubacterium which alternately runs and tumbles and which exhibits exponential distributions of run and tumble lengths (3) and clockwise and counterclockwise interval lengths (4, 5). The key postulate is that the exponential character of the distributions derives from a Poisson process, in which spontaneous transitions between clockwise and counterclockwise rotation occur with a constant probability per unit time (3). In the model illustrated in the rightmost part of the diagram (see Fig. 10), such a stochastic process governs the transition from state N (nonreversing) to state R (reversing) of the switch. To explain the low frequency of short runs, we incorporated a third state of the switch occurring immediately after the reversal (state I [inactive]; see Fig. 10). The switch returns from state R to state N through state I, which produces a ca. 2-s period of low reversal frequency before the state N Poisson rate is restored.

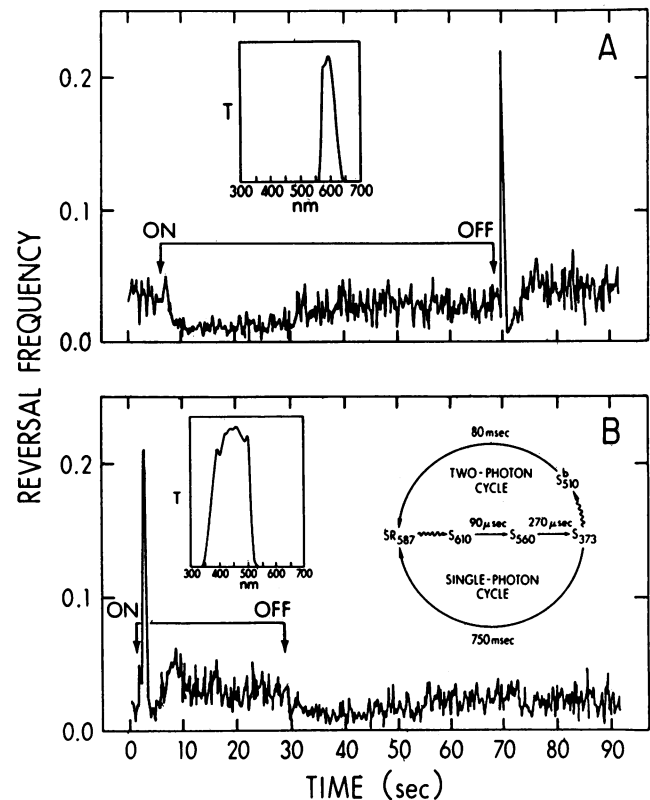


FIG. 2. Reversal frequency responses to photostimuli. Video data were collected at 60 frames per s, and every fourth frame was digitized. Data from three successive points were used to determine reversal frequency (per 200 ms). Attractant light (panel A; 580 to 620 nm, 7.8×10^4 ergs \cdot cm $^{-2}$ \cdot s $^{-1}$; infrared background) or repellent light (panel B; 360 to 520 nm, 3.9×10^3 ergs \cdot cm $^{-2}$ \cdot s $^{-1}$; infrared plus 580- to 620-nm background) was applied at the times indicated. Transmission spectra for filters used to select actinic illumination are shown in the inserts. Insert, upper right-hand corner of panel B: photochemical reaction scheme of SR-I (Bogomolni and Spudich, submitted for publication). Symbols: ~~~~ , light-dependent reactions; — , thermal steps. Subscripts denote absorption maxima of photointermediates.

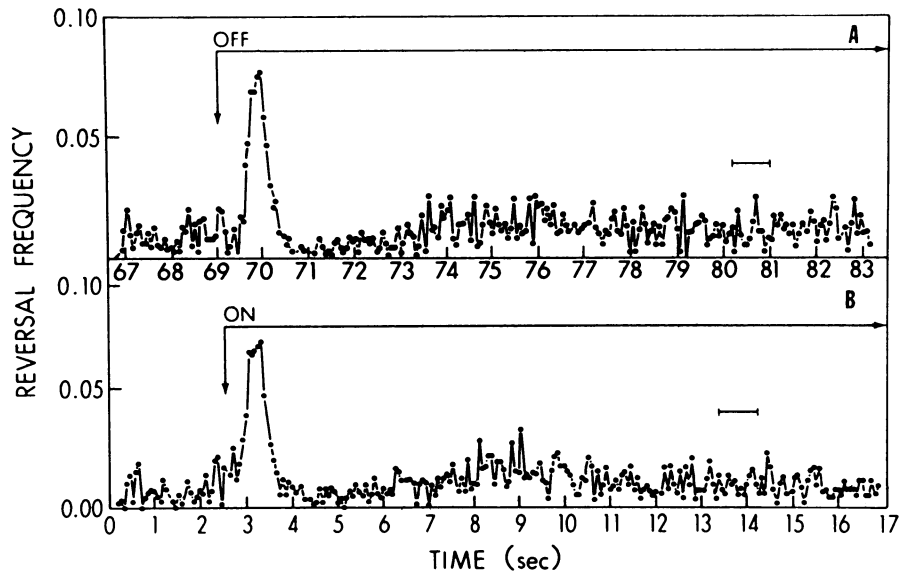


FIG. 3. Reversal induction by SR-I. Video data in the region of the reversal peaks of Fig. 2A and B were collected at 60 frames per s, every fourth frame was digitized, and reversal frequency (per 67 ms) was determined. Bars are drawn at the mean spontaneous run length time (10.5 s) from the stimulus-induced peaks.

Stimulus behavior. The reversal frequency of a population of cells exposed to attractant and repellent light pulses can be monitored by using a computerized tracking system coupled to electronic shutters (28). After an attractant (orange) light is turned on (Fig. 2A; $t = 6$ s) or a repellent (blue) light is turned off (Fig. 2B; $t = 29$ s), the cells exhibit a period of reversal suppression followed by a return to the prestimulus reversal frequency. The opposite stimulus, a decrease in attractant (Fig. 2A, $t = 69$ s) or an increase in repellent light (Fig. 2B, $t = 2.5$ s), triggers a burst of reversals in the population. After several seconds the population regains the prestimulus reversal frequency (adaptation).

Troughs lasting 2 to 3 s appear after the reversal peaks in Fig. 2; this is shown at finer time resolution in Fig. 3. The troughs are predicted by the existence of a state of low reversal probability (i.e., state I) occurring immediately after a reversal. A second prediction of the switch model follows from the stochastic nature of the N-to-R transition. Since the return of reversals after state I depends on a Poisson process, the cells should become randomized (i.e., asynchronous) with respect to the time of occurrence of their next reversals. This is borne out by the data (Fig. 3), which show only a slight transient rise (centered at 75 s [Fig. 3A] and 9 s [Fig. 3B]) in reversal frequency detectable immediately after the trough, indicating that randomization rather than synchronization is the dominant effect.

Responses to stimuli after spontaneous reversals. Since the probability of reversal of the switch is constant after the I state decays, a natural question is whether the responsiveness of the switch to reversal-suppressing and reversal-inducing stimuli is constant as well. To answer this, attractant and repellent stimuli were delivered at various times after occurrence of a spontaneous reversal (Fig. 4). For increases in attractant light, the mean time between stimulus delivery and the next reversal was constant when stimuli were delivered after delays of 0.5 to 7.5 s following a spontaneous reversal. These delays spanned most of the

range of the mean spontaneous reversal interval length, which is 9 s for the cells used in these measurements. We did not observe a decreasing effectiveness of reversal-suppressing stimuli with time after a spontaneous reversal, as was reported in an earlier study (14).

For increases in repellent light, reversal induction occurred with comparable latencies at various times after reversal except for times less than 1.5 s (Fig. 4). A similar refractory period in *H. halobium* was observed by Schimz and Hildebrand (14) and was seen in early work on other phototactic bacteria (7; see references to phototaxis in reference 2). We interpret the refractory period as indicating that the reversal-inducing stimulus is effective only when the switch is in the N state, and the emergence of the cells from the refractory period parallels decay of the I state (see Fig. 10).

From the data shown here (Fig. 4), as well as those shown previously (14), it would appear that the switch is not refractory to the reversal-suppressing stimuli in the period refractory to reversal-inducing stimuli. However, a 1-s pulse of red light, which suppresses reversals for 4 s when delivered at times >2 s following a spontaneous reversal, causes only 1 s of reversal delay when delivered at 1 s after a spontaneous reversal. Therefore the cells are apparently refractory to reversal-suppressing stimuli as well, when these stimuli are delivered as pulses. The apparent asymmetry in refractoriness to sustained increases in attractant light as opposed to repellent light (Fig. 4) probably derives from the slower rate of adaptation to increases in attractant light (compare Fig. 2A and B). Hence by the time the switch reenters state N, adaptation to the repellent light is nearly complete, whereas adaptation to the attractant light, which requires over 20 s (Fig. 2A), has not proceeded to a significant extent. Our interpretation is that the switch is refractory to both reversal-inducing and reversal-suppressing stimuli in the I state (see Fig. 10).

Responses to stimuli after stimulus-induced reversals. A reversal peak was induced by a decrease in orange light at

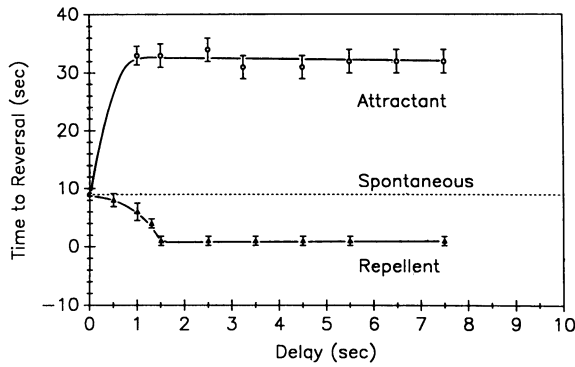


FIG. 4. Effect of stimuli at various times after spontaneous reversal. Attractant (light at 580 to 620 nm) and repellent (light at 360 to 520 nm) stimuli, as in Fig. 2, were delivered at various times after cells exhibited spontaneous reversals (designated time zero). The time from delivery of the stimulus to the next reversal is plotted against the time from the spontaneous reversal to delivery of the stimulus (delay). Mean time to reversal for these cells in the absence of stimuli was 9 s. Cells were monitored with infrared background illumination. Error bars are ± 2 standard errors of the mean for ≥ 30 cells tracked per point.

time zero in Fig. 5 and Fig. 6B to D. Delivery of a blue pulse after the switch had returned to state N induced reversals (Fig. 5A), whereas during the period corresponding to the I state, onset of the same light, delivered as sustained (Fig. 5B) or short (Fig. 5C) pulses, did not produce a reversal peak within the pulse. This confirms the results following spontaneous reversals and, again in the context of our model (see Fig. 10), indicates that the state I of the switch is refractory to reversal-inducing stimuli.

A 1-s pulse of attractant light delivered after a stimulus-induced reversal peak at the same time as the repellent pulse of Fig. 5C caused a second sharp reversal peak (Fig. 6B). A brief period of suppression after the second stimulus preceded the peak (Fig. 6C and D). In the absence of the first stimulus, the effect of such a pulse of orange light was reversal suppression for 3.5 s (Fig. 6A). Since the same orange light stimulus did not induce reversals when delivered after a spontaneous reversal (Fig. 4), an effect of the prior stimulus used to induce the first peak in Fig. 6B must be responsible for the inversion. This effect persisted for at least 6 s, at which time a diminished peak was produced (Fig. 6D). By 12 s after the first stimulus, the orange light pulse regained its reversal-suppressing nature (data not shown). The adaptation system, rather than primary receptor reactions, seems likely as the cause of the inverted response to orange light, since the SR-I receptor signaling form (see below) had decayed to the photochemical ground state of the pigment well within the 6-s period before the stimulus in Fig. 6D.

SR-I signal generation. Measurement of the effect of receptor excitation on the states of the flagellar motor switch, when combined with well characterized specific perturbations of the receptor reactions, can provide information regarding the role of these reactions in signaling. Compelling evidence has established that the reversal-suppressing and reversal-inducing responses to the increase and decrease of attractant light (Fig. 2A) are mediated by the single-photon cycle of SR-I (Fig. 2B, insert) (reviewed in references 21 and 32). Responses to repellent light in the spectral range used in Fig. 2B can result from either the two-photon cycle of SR-I (Fig. 2B, insert) or photoexcitation of SR-II (λ_{max} , 480 nm). Under the conditions used here, SR-II was not detectable in

the cells (retinal-reconstituted Flx3R) either by flash photolysis (assayed as in reference 20) or by behavioral assay (Fig. 7). Illumination (450 nm; Fig. 7C) near the SR-II maximum absorption did not induce reversals, but a comparable intensity of 400-nm light in a red-light background that generates S_{373} was effective (Fig. 7A). The same stimulus shown in Fig. 2B, which spans the SR_{587} and S_{373} absorption spectra and generates the two-photon reaction of SR-I, was effective (Fig. 7B). These results therefore simplify analysis of the responses described below, which can be interpreted in terms of the attractant and repellent reactions of SR-I.

We know that the attractant signal results from the SR-I single-photon photocycle in which SR_{587} is converted to S_{373} , which thermally returns to SR_{587} (22). Various intermediates are generated along the path of formation of S_{373} (Bogomolni and Spudich, submitted). We wanted to know whether the attractant signal was generated with each turn of the cycle (i.e., whether the signal was dependent on the frequency of cycling) or whether the attractant signal was produced by the photointermediate state of the receptor itself (i.e., whether

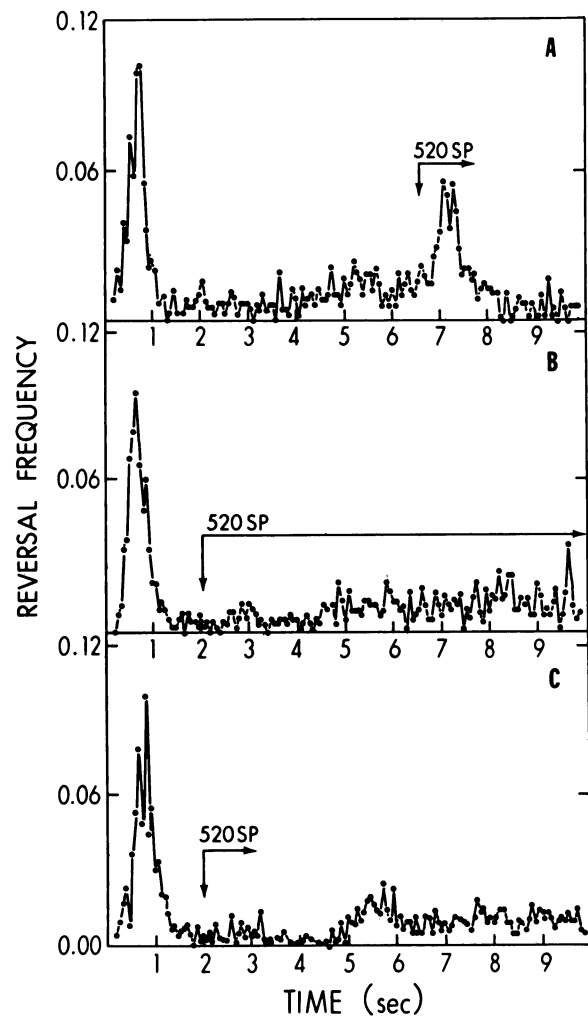


FIG. 5. Double-pulse stimuli: effect of repellent light. Attractant illumination (580 to 620 nm) for 35 s was turned off at time zero, and repellent pulses (360 to 520 nm, labeled 520 SP [shortpass]) were delivered for the times indicated by the arrows. The cycling time for repetitions of the stimulus was 45 s. Reversal frequency was assessed as for Fig. 3.

the signal was dependent on the S_{373} lifetime). We can distinguish between these possibilities by selectively perturbing the decay rate of S_{373} in a manner which decreases the frequency of cycling while increasing the lifetime of S_{373} and examining the effects on SR-I signaling.

Replacement of the native all-*trans*-retinal with retinal analogs perturbs the properties of SR-I (24; McCain et al., *Biophys. J.*, 1986 and 1987). A series of acyclic and ring desmethyl analogs of all-*trans*-retinal synthesized in the laboratory of Koji Nakanishi alter the decay of the S_{373} intermediate in the SR-I photocycle (McCain et al., *Biophys. J.*, 1987). The rates of thermal decay of the analog S_{373} -like intermediates were slowed by one-half to one-eighth the rate

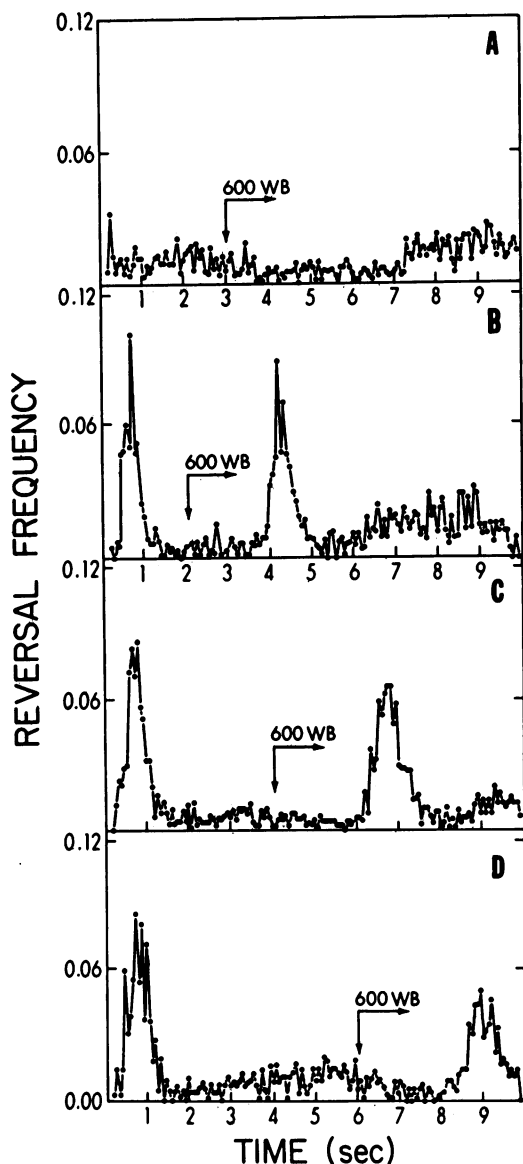


FIG. 6. Double-pulse stimuli: effect of attractant light. (A) Reversal suppression from an attractant pulse. (B to D) The same pulse as in panel A was delivered at various times after a decrease in attractant light at time zero as for Fig. 5. The cycling time for repetitions of the stimulus was 45 s. The reversal frequency was assessed as for Fig. 3.

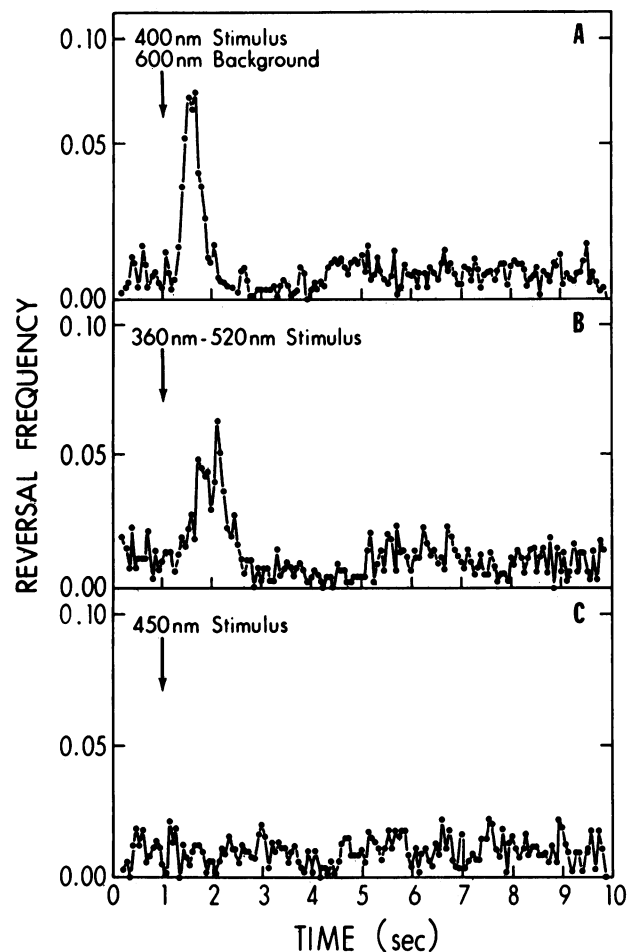


FIG. 7. Test for SR-II contribution to reversal induction. Light was delivered at the time of the arrows and remained on for 9 s. A total of 36 s of background light occurred between successive repetitions of the stimulus. The reversal frequency was determined as for Fig. 3. Photostimuli previously shown (28) to generate repellent responses selectively through SR-I and SR-II were delivered in panels A and C, respectively. The lack of detectable SR-II response at 450 nm indicates that the broad-band stimulus (panel B) is generated by the SR-I two-photon cycle. (A) Light of 400 ± 10 nm, 4.0×10^4 ergs \cdot cm $^{-2}$ \cdot s $^{-1}$, 600-nm background, same illumination designated as 580- to 620-nm background in Fig. 2. (B) Stimulus light as in Fig. 2, infrared background. (C) Light of 450 ± 20 nm, 3.5×10^5 ergs \cdot cm $^{-2}$ \cdot s $^{-1}$, infrared background. For the strain (retinal-reconstituted Flx3R) and conditions used here, no response was detected to the 450-nm stimulus in the absence (C) or presence (data not shown) of the 600-nm background.

of native S_{373} as determined by flash photolysis of cell suspensions at 37°C. The most pronounced effect was observed with the acyclic analog 3,7,11-trimethyl-2,4,6,8-dodecapentaenal (pentaenal). Cells reconstituted with all-*trans*-retinal, the native chromophore, when subjected to an orange flash showed an A_{570} depletion characteristic of SR $_{587}$ photoconversion to S_{373} , and a return of A_{570} due to S_{373} decay with a $t_{1/2}$ of 700 ms (all-*trans*-retinal; Fig. 8A, insert). Flash photolysis of pentaenal-reconstituted SR-I resulted in the formation of an S_{373} -like intermediate with a rise time indistinguishable from that of native SR-I (300 μ s; R. A. Bogomolni, personal communication). The decay of the pentaenal- S_{373} , however, was slowed to a $t_{1/2}$ of 5.5 s

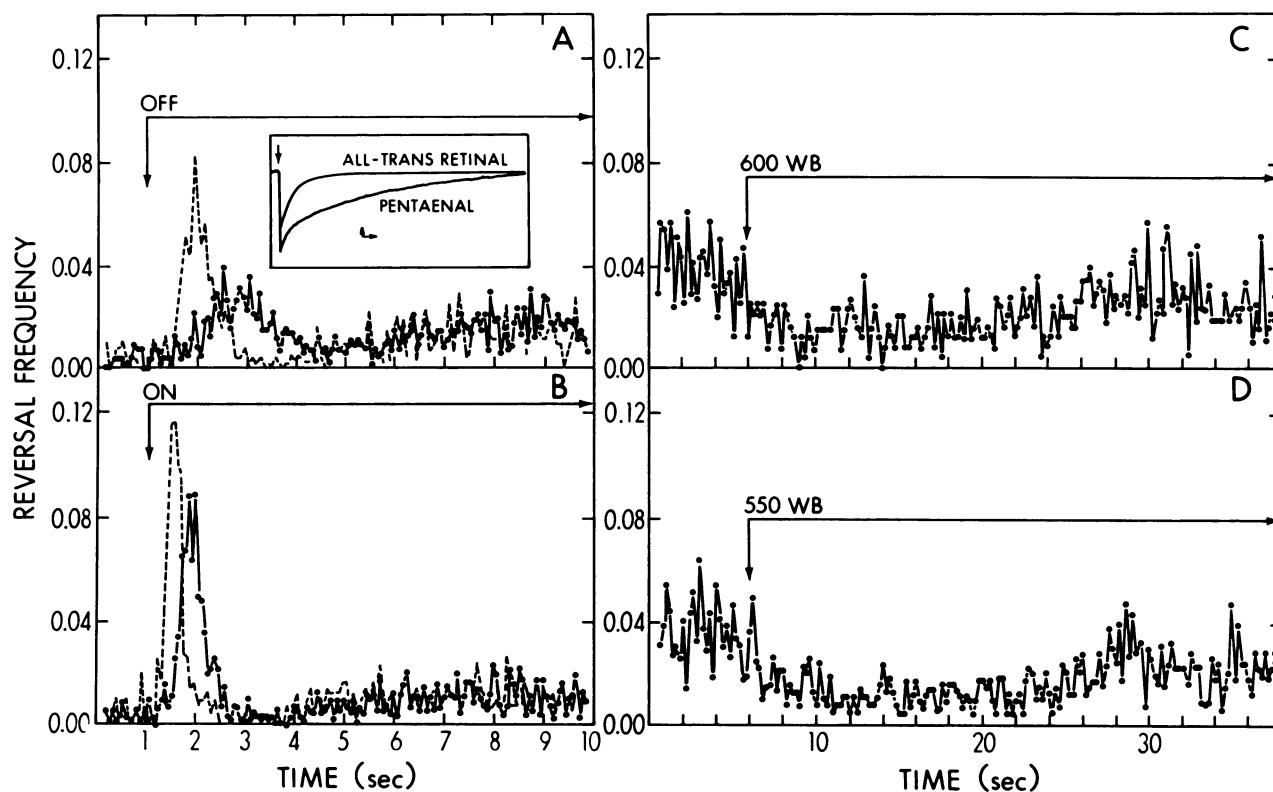


FIG. 8. Reversal frequency responses to photostimulation of pentaenal and all-*trans*-retinal-reconstituted Flx3R. (A) The reversal frequency (per 67 ms) was determined as for Fig. 3 in response to a decrease in light at 580 to 620 nm (----, all-*trans*-retinal) or 530 to 570 nm (—, pentaenal), each at $7.8 \times 10^4 \text{ ergs} \cdot \text{cm}^{-2} \cdot \text{s}^{-1}$. Inset: flash-induced *in vivo* A_{570} changes; 1-ms flash, $\geq 600 \text{ nm}$, delivered at the time indicated by the arrow as described previously (20). Arrows: vertical, 10^{-2} absorbance change; horizontal, 1 s. (B) Responses to increase in light at 360 to 520 nm as in Fig. 2 with the actinic illumination of panel A as a constant background; all-*trans*-retinal (----) and pentaenal (—). (C and D) Reversal suppression from delivery of the attractant lights of panel A to all-*trans*-retinal-reconstituted (C) and pentaenal-reconstituted (D) Flx3R cells. Data were collected at 60 frames per s, and every 12th frame was digitized. Reversal frequency (per 200 ms) was determined without the improved signal-to-noise ratio from the three-point averaging used for Fig. 2.

(pentaenal; Fig. 8A, insert). Analysis of the traces indicated biphasic decay kinetics *in vivo* (data not shown) for both the all-*trans*-retinal and pentaenal-regenerated pigments; this was especially evident in the latter (Fig. 8A, insert).

The pentaenal-SR-I mediated reversal induction responses to step-down of the single-photon cycle (Fig. 8A) as well as to two-photon cycle excitation (Fig. 8B) with a delayed response in both cases compared with native SR-I (Fig. 8A and B, dotted curve). The delayed responses of the pentaenal cells in Fig. 8A could result either from a reduced frequency of cycling of the pentaenal pigment or, alternatively, from the more gradual removal of S_{373} intermediate in the step-down response. To distinguish between these two possibilities another method of analysis is needed, which can be based on suppression responses as described below.

Reversal suppression responses to a step-up in single-photon cycling for the all-*trans*-retinal-SR-I and pentaenal-SR-I are shown in Fig. 8C and D, respectively, for wavelengths adjusted to the absorption maxima of the all-*trans*-retinal-SR-I versus pentaenal-SR-I to yield comparable cycling of both pigments at the intensities used. The length of reversal suppression was determined from similar reversal frequency measurements, as well as from visual cell tracking at various light intensities for the two pigments (Fig. 9). These data demonstrate the concentration of the S_{373} intermediate rather than the frequency of the cycle governs the response, as is clear from the following analysis.

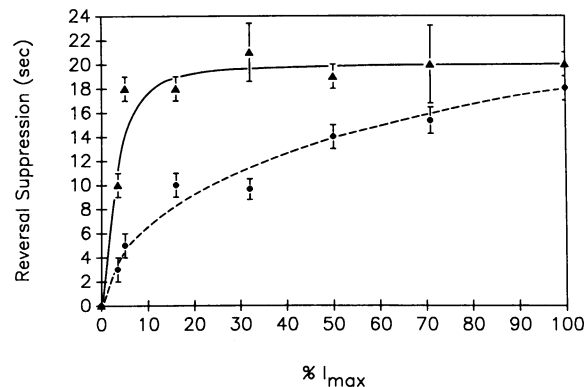


FIG. 9. Reversal suppression response to intensity changes of pentaenal and all-*trans*-retinal-reconstituted Flx3R. Reversal suppression determined as the length of time reversal frequency was below the spontaneous level. All points except those at 32 and 71% I_{\max} were measured from curves such as in Fig. 8C and D for all-*trans*-retinal (●, ----) and pentaenal cells (▲, —) subjected to photostimuli at various intensities of 580 to 620 nm or 530 to 570 nm, respectively. Error bars are $\pm 1 \text{ s}$, estimated as the accuracy in assessing the initial drop from and final rise to the spontaneous level. Points at 32 and 71% were obtained by individual cell tracking, and the length of the error bars is ± 2 standard errors of the mean for ≥ 50 cells. I_{\max} , Intensities in Fig. 8.

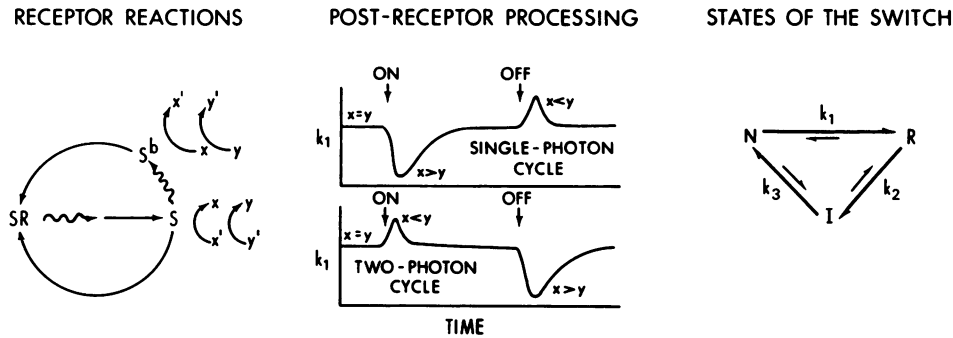


FIG. 10. Model for the flagellar motor switch and its modulation by SR-I. Kinetic properties of the switch and receptor coupling are based on the measurements presented here. States of the switch are nonreversing (N), reversing (R), and inactive (I) and are related kinetically as shown. A unidirectional bias in the transitions between states requiring energy input is implicitly assumed. Receptor states designated SR, S, and S^b represent SR_{587} , S_{373} , and S^b_{510} , respectively (23). In the model, postreceptor processing is proposed to induce a transient perturbation in the rate constant k_1 . Reduction in k_1 decreases the probability of the N-to-R transition. k_1 is dependent on the relative values of signals x and y , x being controlled by the receptor states and y being controlled by the adaptation system. The leftmost section indicates the S intermediate favoring excitation signal (x) generation and, through an unspecified pathway, the counterbalancing adaptation signal (y). Since two-photon cycling causes the opposite responses as single-photon cycling, the opposing reactions are shown favored by the two-photon product, S^b_{510} .

The photostationary state concentration of the S_{373} intermediates (S) of both all-*trans*-retinal-SR-I and pentaenal-SR-I is $S = (k_f \cdot SR_0)/(k_f + k_d)$, where SR_0 is the total amount of SR-I reconstituted, k_f is the rate constant of formation of the S intermediate, which is proportional to the light intensity and is equal for both pigments under the conditions of our measurements, and k_d is the thermal decay rate constant of the S intermediate. Although neither pigment exhibits simple first-order kinetics, to a first approximation $k_d(\text{pentaenal}) = k_d(\text{all-trans})/8$.

The frequency F of photocycling for both pigments is $F = k_f \cdot k_d \cdot SR_0/(k_f + k_d)$. At high light intensities at which $k_f \gg k_d$, $S = SR_0$ and $F = k_d SR_0$. Therefore, since the two pigments differ only in k_d , if the response is governed by flux through the cycle (i.e., the frequency of cycling, F), at high light intensities the pentaenal response should be only one-eighth of the all-*trans*-retinal response, contrary to our observation (Fig. 9). Alternatively, if the response is dependent on S , the all-*trans*-retinal and pentaenal fluorescence-response curves should approach the same value at high fluence, which is what we observe (Fig. 9).

At low light intensities at which $k_f \ll k_d$, $S = k_f SR_0/k_d$ and $F = k_f SR_0$. Therefore, if the response depends on the frequency of cycling, the two pigments should generate the same suppression at low intensities, again contrary to our observations (Fig. 9). Alternatively, if the response is governed by S , the pentaenal response should be greater than that of all-*trans*-retinal-reconstituted cells, which is what we observe (Fig. 9).

These results indicate that attractant signaling is governed by the accumulation of the SR-I photointermediates. The longer lifetime of the pentaenal- S_{373} is correlated with a longer period of reversal suppression, even though the frequency of cycling, and therefore the rates of all reactions in the cycle, are reduced in the pentaenal pigment.

DISCUSSION

States of the switch. Our results indicate that a stochastic process governs spontaneous reversing by the flagellar motor of *H. halobium*. We interpret our data in terms of a three-state model of the switch (Fig. 10). State N (non-

versing) undergoes a transition to state R (reversing) via a process having constant probability per unit time, similar to the flagellar motor in *E. coli* (3). The switch returns to state N, passing through an intermediate nonreversing state I (inactive), which is evident as a ca. 2-s period of low reversal frequency after spontaneous or stimulus-induced reversals. In stochastic process theory, this can be described mathematically as a renewal process in which the resultant distributions of run times is a convolution of blocked times (i.e., times during which reversal probability is near zero), with the exponential distribution deriving from the Poisson events (8).

The three-state model of the switch suggested by the spontaneous run time distributions is supported by reversal frequency data from stimulus-induced conditions. Two predictions of the model were tested as follows by photoinduction of a large population of cells to reverse synchronously.

(i) According to the model, after synchronous reversal of a population of cells, nearly all flagellar motor switches will be in state I. Therefore a period of ca. 2 s should occur after the reversal peak during which the population reversal frequency is near zero. This was borne out by the stimulus-induced reversal frequency measurements. After strong stimuli for which >90% of the cells underwent synchronous reversals within a period of <1 s, a 2- to 3-s depression in the frequency occurred immediately following the reversal peak (Fig. 2 and 3).

(ii) A second prediction follows from the stochastic nature of the N-to-R transition. Since the return of reversals after state I depends on a Poisson process, the cells should become randomized (i.e., asynchronous) with respect to the time of occurrence of their next reversals. Conversely, if the occurrence of reversals following the stimulus-induced reversals were not stochastic, then one would expect the cells to exhibit synchrony in their first spontaneous reversal, producing a second reversal peak (possibly but not necessarily at the mean spontaneous run length indicated by the bar in Fig. 3A and B). Only a slight transient rise in reversal frequency immediately after the trough was detectable, indicating that randomization rather than synchronization is the dominant effect.

The second prediction provides an independent test of the postulate that the exponential character of the distributions

in Fig. 1 derives from a Poisson process. The asynchronization observed and the form of the spontaneous run length distributions provide strong evidence that a stochastic process governs the reversal of rotation direction in *H. halobium*, rather than a deterministic process as has been suggested (14). A key difference in our observations compared with those which suggested the deterministic model (14) is that we did not detect a change of responsiveness to either attractant or repellent stimuli with time after a spontaneous reversal (Fig. 5). Accordingly, we find that a model with a Poisson process dominating the occurrence of reversals describes our data most clearly.

Stochastic switching occurs also in the *E. coli* flagellar motor (2-5; 16). There is, however, an important basic difference. In *E. coli* one sense of rotation (counterclockwise) corresponds to smooth swimming, while the other (clockwise) corresponds to tumbling, the mechanism of reorientation of these bacteria. In general, switching between these two states occurs at two different Poissonian rates. Attractant stimuli stabilize the *E. coli* motor in a counterclockwise-rotating sense, and repellents stabilize it in a clockwise-rotating sense. On the other hand, in *H. halobium* there is no attractant- or repellent-induced rotation sense. Rather, it is the switching between rotation senses which is modulated by stimuli. Further, a single Poissonian rate constant appears to govern spontaneous switching from either rotational sense. Accordingly, it is especially useful to analyze sensory regulation of the *H. halobium* motor in terms of its switching properties rather than its sense of rotation per se.

Modulation of the switch. We observe that when the switch is in state I, the cells are refractory to both reversal-inducing and reversal-suppressing stimuli. Our interpretation is that the switch in state I is refractory to receptor signals. Therefore a good candidate for a site of action of these signals is the rate constant k_1 (Fig. 10), which does not influence the switch behavior when the switch is in state I. Reversal-inducing stimuli would transiently increase the value of k_1 , and reversal-suppressing stimuli would transiently decrease the value of k_1 , thereby producing the observed changes in reversal probability.

The transient nature of the changes in k_1 presumes a signal adaptation system between the receptor and the switch. For the sake of discussion it is useful to define the adaptation process in terms of a counterbalancing signal (i.e., a signal with the opposite effect to that of the receptor signal on k_1). This is shown in the middle section of Fig. 10, where x is defined as the excitation signal which alters k_1 and y is the counterbalancing adaptation signal which returns k_1 to its prestimulus value. x and y are not explicitly defined in the model. Working hypotheses are, for x , a metabolite or protein molecule released cytoplasmically by the receptor and, for y , a change in receptor or subsequent component properties by methylation (13) as occurs in eubacteria (17).

Stock et al. have described a three-state kinetic model for receptor signaling and adaptation operating at the receptor level in eubacterial chemotaxis (26). It is important to recognize the distinction that the Stock et al. model applies at the receptor input end of the system, whereas our model, although kinetically similar, describes the switch output kinetics (Fig. 10).

The inverted response to orange light (Fig. 6B to D) following a prior SR-I attractant light step-down stimulus apparently derives from an influence of postreceptor steps of the first stimulus, since the SR-I photointermediates decayed to the photochemical ground state of the pigment within the

6-s period before the second stimulus was applied in Fig. 6D. Furthermore, in another strain (Flx15), which contains both SR-I and SR-II, a step-down in SR-I attractant light (same as delivered at time zero; Fig. 6) inverts the effects of a step down in SR-II-repellent light (450 nm), converting this stimulus from reversal-suppressing to reversal-inducing (data not shown). This further indicates that postreceptor reactions are responsible for the inversion. Although the mechanism for the inversion is not known, possibly incomplete deadaptation to the attractant light step down at time zero results in a higher value of y (Fig. 10) at the time of the second pulse, accentuating the net increase of y , the counterbalancing signal to x , as a result of the pulse, and giving a net opposite (i.e., y -dominated) response.

Receptor reactions. Pentaenal-SR-I which has a lower frequency of photocycling than native all-*trans*-retinal-SR-I owing to a prolonged lifetime of the pentaenal-S₃₇₃ intermediate, is more effective in generating attractant reversal-suppressing signals. This result eliminates any model in which signal generation is coupled to the frequency of cycling. Hence the alternative type of mechanism, in which conformational states of the receptor generate signals to the motor switch, is supported by our results. In this sense, SR-I is similar to rhodopsin, whose functioning depends on a photoproduct (Meta-II [27]). This result is incorporated in our model as a modulation of k_1 by processes initiated by the S₃₇₃ form of SR-I. As is to be expected from its different function, bacteriorhodopsin, although similar to SR-I in biochemical and spectroscopic properties (24; Bogomolni and Spudich, submitted for publication), differs fundamentally from SR-I in that an increase in the lifetime of its S₃₇₃-like intermediate (M₄₁₂) inhibits its proton transport function (10, 12).

ACKNOWLEDGMENTS

We greatly appreciate stimulating discussions with Shahid Khan and Elena Spudich. We also thank Howard Berg, Roberto Bogomolni, Walther Stoeckenius, and Steven Sundberg for their critical reading of the manuscript, and Koji Nakanishi and V. J. Rao for their generous gift of pentaenal.

This work was supported by Public Health Service grants GM27750 and GM34283 from the National Institutes of Health and grant DMB-8416123 from the National Science Foundation Biological Instrumentation Program (to J.L.S.). D.A.M. was supported by Training Grant T32 AM07513 from the National Institutes of Health.

ADDENDUM IN PROOF

After this paper had been submitted, W. Marwan and D. Oesterhelt (J. Mol. Biol. 195:333-342, 1987) reported a distribution of rotational intervals in unstimulated cells that was similar to the distributions in our Fig. 1. They also interpret their results in terms of probabilistic motor switching.

LITERATURE CITED

1. Alam, M., and D. Oesterhelt. 1984. Morphology, function and isolation of halobacterial flagella. J. Mol. Biol. 176:459-475.
2. Berg, H. C. 1975. Chemotaxis in bacteria. Annu. Rev. Biophys. Bioengr. 4:119-136.
3. Berg, H. C., and D. A. Brown. 1972. Chemotaxis in *Escherichia coli* analysed by three-dimensional tracking. Nature (London) 239:500-504.
4. Berg, H. C., and M. Tedesco. 1975. Transient response to chemotactic stimuli in *Escherichia coli*. Proc. Natl. Acad. Sci. USA 72:3235-3239.
5. Block, S. M., J. E. Segall, and H. C. Berg. 1982. Impulse responses in bacterial chemotaxis. Cell 31:215-226.

6. **Bogomolni, R. A., and J. L. Spudich.** 1982. Identification of a third rhodopsin-like pigment in phototactic *Halobacterium halobium*. *Proc. Natl. Acad. Sci. USA* **79**:6250–6254.
7. **Clayton, R. K.** 1953. Studies in the phototaxis of *Rhodospirillum rubrum*. III. Quantitative relations between stimulus and response. *Arch. Mikrobiol.* **19**:141–165.
8. **Cox, D. R., and H. D. Miller.** 1965. The theory of stochastic processes, p. 340–342. Methuen and Co Ltd., London.
9. **Dencher, N. A.** 1983. The five retinal-protein pigments of halobacteria: bacteriorhodopsin, halorhodopsin, P565, P370, and slow-cycling rhodopsin. *Photochem. Photobiol.* **38**:753–767.
10. **Gartner, W., P. Towner, H. Hopf, and D. Oesterhelt.** 1983. Removal of methyl groups controls the activity of bacteriorhodopsin. *Biochemistry* **22**:2673–2644.
11. **Hildebrand, E., and A. Schimz.** 1987. Role of the response oscillator in inverse responses of *Halobacterium halobium* to weak light stimuli. *J. Bacteriol.* **169**:254–259.
12. **Mao, B., R. Govindjee, T. G. Ebrey, M. Arnaboldi, V. Balogh-Nair, K. Nakanishi, and R. Crouch.** 1981. Photochemical and functional properties of bacteriorhodopsins formed from 5,6-dihydro and 5,6-dihydrodesmethylretinals. *Biochemistry* **20**:428–435.
13. **Schimz, A.** 1981. Methylation of membrane proteins is involved in chemosensory and photosensory behavior of *Halobacterium halobium*. *FEBS Lett.* **125**:205–207.
14. **Schimz, A., and E. Hildebrand.** 1985. Response regulation and sensory control in *Halobacterium halobium* based on an oscillator. *Nature (London)* **317**:641–643.
15. **Schimz, A., and E. Hildebrand.** 1986. Entrainment and temperature dependence of the response oscillator in *Halobacterium halobium*. *J. Bacteriol.* **166**:689–692.
16. **Segall, J. E., S. M. Block, and H. C. Berg.** 1986. Temporal comparisons in bacterial chemotaxis. *Proc. Natl. Acad. Sci. USA* **83**:8987–8991.
17. **Springer, M. S., M. F. Goy, and J. Adler.** 1979. Protein methylation in behavioral control mechanisms and in signal transduction. *Nature (London)* **280**:279–284.
18. **Spudich, E. N., and J. L. Spudich.** 1982. Control of transmembrane ion fluxes to select halorhodopsin-deficient and other energy transduction mutants of *Halobacterium halobium*. *Proc. Natl. Acad. Sci. USA* **79**:4308–4312.
19. **Spudich, E. N., and J. L. Spudich.** 1982. Measurement of light-regulated phosphoproteins of *Halobacterium halobium*. *Methods Enzymol.* **88**:213–216.
20. **Spudich, E. N., S. A. Sundberg, D. Manor, and J. L. Spudich.** 1986. Properties of a second sensory receptor protein in *Halobacterium halobium* phototaxis. *Proteins* **1**:239–246.
21. **Spudich, J. L.** 1984. Genetic demonstration of a sensory rhodopsin in bacteria, p. 221–229. *In* E. Helmreich, L. Bolis, and H. Passow (ed.), *Information and energy transduction in biological membranes*. Alan R. Liss, Inc., New York.
22. **Spudich, J. L., and R. A. Bogomolni.** 1983. Spectroscopic discrimination of the three rhodopsinlike pigments in *Halobacterium halobium* membranes. *Biophys. J.* **43**:243–246.
23. **Spudich, J. L., and R. A. Bogomolni.** 1984. Mechanism of colour discrimination by a bacterial sensory rhodopsin. *Nature (London)* **312**:509–513.
24. **Spudich, J. L., D. A. McCain, K. Nakanishi, M. Okabe, N. Shimizu, H. Rodman, B. Honig, and R. A. Bogomolni.** 1986. Chromophore/protein interaction in bacterial sensory rhodopsin and bacteriorhodopsin. *Biophys. J.* **49**:243–246.
25. **Spudich, J. L., and W. Stoerkenius.** 1979. Photosensory and chemosensory behavior of *Halobacterium halobium*. *J. Photobiophys.* **1**:43–53.
26. **Stock, J., G. Kersulis, and D. E. Koshland, Jr.** 1985. Neither methylating nor demethylating enzymes are required for bacterial chemotaxis. *Cell* **42**:683–690.
27. **Stryer, L.** 1986. Cyclic GMP cascade of vision. *Annu. Rev. Neurosci.* **9**:87–119.
28. **Sundberg, S. A., M. Alam, and J. L. Spudich.** 1986. Excitation signal processing times in *Halobacterium halobium* phototaxis. *Biophys. J.* **50**:895–900.
29. **Sundberg, S. A., R. Bogomolni, and J. L. Spudich.** 1985. Selection and properties of phototaxis-deficient mutants of *Halobacterium halobium*. *J. Bacteriol.* **164**:282–287.
30. **Takahashi, T., and Y. Kobatake.** 1982. Computer-linked automated method for measurement of the reversal frequency in phototaxis of *Halobacterium halobium*. *Cell Struct. Funct.* **7**:183–192.
31. **Takahashi, T., Y. Mochizuki, N. Kamo, and Y. Kobatake.** 1985. Evidence that the long-lifetime photointermediate of s-rhodopsin is a receptor for negative phototaxis in *Halobacterium halobium*. *Biochem. Biophys. Res. Commun.* **127**:99–105.
32. **Takahashi, T., H. Tomioka, N. Kamo, and Y. Kobatake.** 1985. A photosystem other than PS370 also mediates the negative phototaxis of *Halobacterium halobium*. *FEMS Microbiol. Lett.* **28**:161–164.
33. **Tomioka, H., N. Kamo, T. Takahashi, and Y. Kobatake.** 1984. Photochemical intermediate of third rhodopsin-like pigment in *Halobacterium halobium* by simultaneous illumination with red and blue light. *Biochem. Biophys. Res. Commun.* **123**:989–994.
34. **Tomioka, H., T. Takahashi, N. Kamo, and Y. Kobatake.** 1986. Flash spectrophotometric identification of a fourth rhodopsin-like pigment in *Halobacterium halobium*. *Biochem. Biophys. Res. Commun.* **139**:389–395.
35. **Wolff, E., R. A. Bogomolni, P. Scherrer, B. Hess, and W. Stoerkenius.** 1986. Color discrimination in halobacteria: spectroscopic characterization of a second sensory receptor covering the blue-green region of the spectrum. *Proc. Natl. Acad. Sci. USA* **83**:7272–7276.